

25 model are, in many cases, below current precision. Therefore, the possible
26 path for the search of the new physics is to reveal the deviations in the
27 measurement of the observables that are sensitive to the presence of these
28 phenomena. One of the proposed high precision machines is the electron-
29 positron collider ILC (International Linear Collider). The important part
30 of the physics program at ILC are the precise measurements of the Higgs
31 boson properties, at the first place the measurements of its couplings. The
32 Standard model predicts strict linear dependence as the function of masses
33 of corresponding particles. The shape and the nature of the eventual devi-
34 ations of the couplings can signify the proposed model of the new physics.
35 The precision of the coupling measurements of an order of few percents is
36 needed to be sensitive to these deviations [1].

37
38 The ILC physics case of 250 GeV has been elaborated in detail [2] and
39 the comprehensive set of studies of the foreseen physics program have been
40 performed in full simulation [3]. It was shown that the necessary sensitiv-
41 ity can be successfully achieved at ILC collider.

42
43 The talk presents the results of the measurement of the Higgs decay
44 into a pair of W bosons, at the nominal center-of-mass energy, 250 GeV
45 of ILC, using Higgstrahlung as Higgs production process. The relative
46 statistical accuracy of the measurement of the $\sigma(HZ) \times BR(H \rightarrow WW^*)$,
47 allowing the extraction of the precision of $\frac{g_{HZZ}^2 g_{HWW}^2}{\Gamma}$.

48 2 Simulation and analysis tools

49 A common linear collider software package, ILCSoft, is used. Signal and
50 background samples are simulated using the Whizard 1.95 [4] event gener-
51 ator, including initial state radiation and a realistic luminosity spectrum.
52 The hadronisation and fragmentation of the Higgs and vector bosons were
53 simulated using Pythia 6.4 [5]. For the completeness, $\gamma\gamma$ to hadrons back-
54 ground, although negligible at this energy stage, is overlaid over each gen-
55 erated event sample before reconstruction. Particle reconstruction and
56 identification was done using the particle flow technique, implemented in
57 the Pandora particle-flow algorithm (PFA) [7, 8]. The ILD_o1_v05 detector
58 model is used.

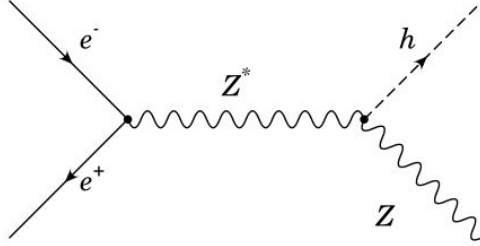


Figure 1: Left: The Feynman diagram of the dominant Higgs production processes (Higgsstrahlung).

Table 1: List of considered background processes, with the corresponding cross-sections, preselection and final selection efficiency. The last column gives the number of events in the final sample. The $\sqrt{s} = 250$ GeV with integrated luminosity of 500fb^{-1} is assumed.

Process	$\sigma[\text{fb}]$	ϵ_{pres} [%]	ϵ_{tot} [%]	evts_{fin}
signal	36.5	89.2	30.0	5600
other Higgs decays	309.8	54.7	4.1	6338
$e^+e^- \rightarrow 2f$ hadronic	129148.6	1.5	$< 10^{-2}$	5410
$e^+e^- \rightarrow 4f$ WW hadronic	14874.3	33.5	0.2	14961
$e^+e^- \rightarrow 4f$ WW/ZZ hadronic	12383.3	33.8	0.2	13340
$e^+e^- \rightarrow 4f$ ZZ hadronic	1402.0	42.9	1.0	7178
$e^+e^- \rightarrow 4f$ WW semileptonic	18781.0	0.5	$< 10^{-5}$	/
$e^+e^- \rightarrow 4f$ ZZ semileptonic	1422.1	$5 \cdot 10^{-4}$	$< 10^{-2}$	49

59 3 Event samples

60 The staged concept of ILC [9], foresees the first stage at $\sqrt{s} = 250$ GeV.
 61 The dominant Higgs production channel is the Higgsstrahlung, with the
 62 cross section of 346 fb, including the maximal left beam polarization of
 63 $(e^-, e^+) = (-80\%, +30\%)$. The Feynman diagram of the Higgsstrahlung
 64 Higgs production channel is shown in the Figure 1.

65 The analyzed signal events are fully hadronic, where all the bosons in the
 66 event, the Z boson, as well as both W bosons decay hadronically. The
 67 corresponding signal cross-section is 36.5 fb. The signal and background
 68 processes that are considered are listed in the Table 1.

69 4 Event selection

70 The events are clustered into six jets the k_T clustering algorithm. The
71 b and c-tagging probabilities, as determined by LCFIPlus package, are
72 assigned to each jet in the event, for both, six-jet and additional two-jet
73 hypothesis. In the next step, the signal process is reconstructed by the
74 jet pairing to form candidates for the Z boson and one on-shell and one
75 off-shell W boson, which are coming from Higgs decay. The combination
76 of the pairs of jets, for which the following χ^2 has a minimum, is chosen:

$$\chi^2 = \frac{m_{ij} - m_W}{\sigma_W^2} + \frac{m_{kl} - m_Z}{\sigma_Z^2} + \frac{m_{ijmn} - m_H}{\sigma_H^2}$$

77 where m_{ij} , m_{kl} are the invariant masses of a di-jet pairs, which are assigned
78 to the real W and the Z boson candidates, while m_{ijmn} is the invariant mass
79 of the jets that comprize the Higgs boson candidate. m_V and σ_V , ($V =$
80 W, Z, H), are the masses and the widths of the corresponding bosons.

81 The jet-opening of the clustered jets was optimized according to the
82 criteria of minimal widths and the closest reconstructed mean of the re-
83 constructed dijet mass distributions to that of the Z and the real W boson.
84 The best results are obtained with the jet opening of $R=1.5$.

85 The cross-sections of the considered background processes are several
86 orders of magnitude higher than for the signal events (Table 1), therefore
87 at the next step, the background to signal ratio is minimized by the set of
88 preselection criteria prior to the final selection. The list of the preselection
89 variables with the corresponding cut-off values:

- 90 • the invariant mass of the Z boson candidate , $m_Z > 70$ GeV,
- 91 • the invariant mass of the Higgs boson candidate , $m_H > 100$ GeV,
- 92 • the invariant mass of the real W boson candidate, $m_W > 60$ GeV,
- 93 • number of particle flow objects, $NPFO > 70$,
- 94 • visible energy, $E_{vis} > 200$ GeV,
- 95 • transverse momentum of a single jet, $p_T < 20$ GeV,
- 96 • event thrust < 0.9 ,
- 97 • $-\log(y_{45}) < 2.2$, $-\log(y_{56}) < 3.0$, $-\log(y_{45}) < 4.4$, $-\log(y_{56}) < 4.8$,

98 where $-\log(y_{ij})$ is k_T value at which the jet number is making the transition
 99 from the i -th to the j -th number of jets in the event.

100 The efficiencies of reduction by the preselection are given in Table 1 for
 101 signal and background processes.

102 The final event selection is achieved using the multivariate analysis
 103 method, Boosted decision tree (BDT). The set of training background
 104 samples, as well as the set of input variables, are optimized. The final
 105 event selection is performed using purely hadronic background with the
 106 following discriminating input variables:

- 107 • the invariant masses of both W bosons, Z and Higgs boson, m_W , m_Z ,
 108 m_H ,
- 109 • number of particle-flow objects (NPFO) in the event,
- 110 • transverse momentum of jets that comprize the Higgs boson, p_T^{Higgs} ,
- 111 • the highest transverse momentum of a jet in the event, p_T^{max} ,
- 112 • jets transitions $-\log(y_{12})$, $-\log(y_{23})$, $-\log(y_{34})$, $-\log(y_{45})$, $-\log(y_{56})$, -
 113 $\log(y_{67})$,
- 114 • event shape variables (thrust, oblatness, sphericity and aplanarity),
- 115 • and second highest flavor tagging probabilities for the two jet hy-
 116 pothesis (btag, ctag),
- 117 • angle that comprize the Z boson,
- 118 • angle that comprize the real W boson.

119 The classifier cut value of the final selection, is chosen to minimize the
 120 statistical uncertainty of the cross-section $\sigma(HZ) \times BR(H \rightarrow WW^*)$, that
 121 is to minimize the ratio

$$\frac{\Delta\sigma}{\sigma} = \frac{N_S}{\sqrt{(N_S + N_B)}}, \quad (1)$$

122 where N_S , N_B are the number of signal and background events after the
 123 final selection, respectively. The relative statistical uncertainty of the prod-
 124 uct of the Higgsstrahlung cross-section and the corresponding branching
 125 ratio is calculated as:

126 The number of signal and background events after the final selection
 127 are given in the Table 1.

128 5 Conclusion

129 In this talk, the measurement accuracy, $\Delta(\sigma \cdot BR)/(\sigma \cdot BR)$, of the Higgs
130 decay to a W pair is presented. Fully hadronic final states is considered.
131 The study is performed at the first energy stage of the ILC, $\sqrt{s} = 250$
132 GeV, using Higgsstrahlung Higgs production channel. The assumed beam
133 polarization is $P(e^-, e^+) = (-80\%, +30\%)$, with the integrated luminosity
134 of 500 fb^{-1} and the mass of Higgs boson of 125 GeV. The signal and
135 background events are fully simulated, including initial state radiation and
136 beam induced background.

137 The obtained result for the relative statistical uncertainty of the $\sigma(HZ) \cdot$
138 $BR(H \rightarrow WW^*)$ is 4.1%. This particular measurement is important for
139 model independent determination of Higgs total width, and therefore for
140 global fit, and it has been shown that this result improves the total Higgs
141 decay width by of approximately 10%.

142 References

- 143 [1] T. Barklow, K. Fujii, S. Jung, R. Karl, J. List, T. Ogawa, M. Pe-
144 skin, J. Tian, Improved Formalism for Precision Higgs Coupling Fits,
145 Phys.Rev. D97 (2018) no.5, 053003.
- 146 [2] K. Fujii et al, [LCC Physics Working Group], Physics Case for the 250
147 GeV Stage of the International Linear Collider, arXiv:1710.07621v4
148 [hep-ex] 7 Aug 2017.
- 149 [3] LCWS16, Proceedings of International Workshop on Future Lin-
150 ear Colliders 2016 (LCWS2016) : Morioka, Iwate, Japan, De-
151 cember 05-09, 2016, <http://www.slac.stanford.edu/econf/C1612054/>
152 Proceedings of International Workshop on Future Linear Col-
153 liders 2017 (LCWS2017), Strasbourg, France, 23-27 Oct 2017,
154 <http://inspirehep.net/record/1614364>
- 155 [4] W. Kilian, T. Ohl and J. Reuter, WHIZARD: Simulating Multi-
156 Particle Processes at LHC and ILC, Eur. Phys. J. C 71 (2011) 1742,
157 DOI : 10.1140/epjc/s10052-011-1742-y.
- 158 [5] T. Sjostrand, S. Mrenna and P.Z. Skands, Pythia, JHEP 0605 (2006)
159 026, DOI : 0.1088/1126-6708/2006/05/026.

- 160 [6] D. Schulte, Beam-beam simulations with GUINEA-PIG, CERN-PS-
161 99-014-LP, 1999.
- 162 [7] M. Thomson, Particle flow calorimetry and the Pan-
163 doraPFA algorithm, Nucl. Instrum. Meth,A 611,
164 2009,doi:10.1016/j.nima.2009.09.009.
- 165 [8] J. Marshall, A. Münnich. Thomson, Performance of particle flow
166 calorimetry at CLIC, Journal of Physics: Conference Series,700, 2012,
167 doi: 10.1016/j.nima.2012.10.038.
- 168 [9] Linear Collider Collaboration,Editors:L. Evans and S. Michizono,
169 The International Linear Collider Machine Staging Report,
170 arXiv:1711.00568.
- 171 [10] A. Hoecker et al, TMVA-Toolkit for Multivariate Data Analysis,
172 arXiv:physics/0703039.
- 173 [11] M. Pandurovic, Measurement of Higgs decay to WW^* in Hig-
174 gsstrahlung at $\sqrt{s}=500$ GeV ILC and in WW -fusion at $\sqrt{s}=3$ TeV
175 CLIC, Proceedings of International Workshop on Future Linear Col-
176 liders 2016 (LCWS2016) : Morioka, Iwate, Japan, December 05-09,
177 2016, arXiv:1703.08871